THE UNIVERSITY *of* EDINBURGH

Edinburgh Research Explorer

Quenching of the N=32 neutron shell closure studied via precision mass measurements of neutron-rich vanadium isotopes

OPEN ACCESS

Quenching of the $N = 32$ neutron shell closure studied via precision mass measurements of neutron-rich vanadium isotopes

M. P. Reiter,[1,2,*] S. Ayet San Andrés,[1,3] E. Dunling,[2,4] B. Kootte,[2,5] E. Leistenschneider,[2,6] C. Andreoiu,[7] C. Babcock,[2]
B. R. Barquest,[2] J. Bollig,[2,8] T. Brunner,[2,9] I. Dillmann,[2,10] A. Finlay,[2,6] G. Gwinner,[5] L. Graham,[2] J. D. Holt,[2] C. Hornung,[1]
C. Jesch,[1] R. Klawitter,[2,11] Y. Lan,[2,6] D. Lascar,[2,12] J. E. McKay,[2,10] S. F. Paul,[2,8] R. Steinbrügge,[2,†] R. Thompson,[13]
J. L. Tracy, Jr.,[2] M. E. Wieser,[13] C. Will,[1] T. Dickel,[1,3] W. R. Plaß,[1,3] C. Scheidenberger,[1,3]
A. A. Kwiatkowski,[2,10] and J. Dilling[2,6]

[1]*II. Physikalisches Institut, Justus-Liebig-Universität, 35392 Gießen, Germany*
[2]*TRIUMF, 4004 Wesbrook Mall, Vancouver, British Columbia V6T 2A3, Canada*
[3]*GSI Helmholtzzentrum für Schwerionenforschung GmbH, Planckstraße 1, 64291 Darmstadt, Germany*
[4]*Department of Physics, University of York, York YO10 5DD, United Kingdom*
[5]*Department of Physics and Astronomy, University of Manitoba, Winnipeg, Manitoba R3T 2N2, Canada*
[6]*Department of Physics and Astronomy, University of British Columbia, Vancouver, British Columbia V6T 1Z1, Canada*
[7]*Department of Chemistry, Simon Fraser University, Burnaby, British Columbia V5A 1S6, Canada*
[8]*Ruprecht-Karls-Universität Heidelberg, D-69117 Heidelberg, Germany*
[9]*Physics Department, McGill University, H3A 2T8 Montréal, Québec, Canada*
[10]*Department of Physics and Astronomy, University of Victoria, Victoria, British Columbia V8P 5C2, Canada*
[11]*Max-Planck-Institut für Kernphysik, Heidelberg D-69117, Germany*
[12]*Center for Fundamental Physics, Northwestern University, Evanston, Illinois 60208, USA*
[13]*Department of Physics and Astronomy, University of Calgary, Calgary, Alberta T2N 1N4, Canada*

We performed the first direct mass measurements of neutron-rich vanadium $^{52-55}$V isotopes passing the $N = 32$ neutron shell closure with TRIUMF's Ion Trap for Atomic and Nuclear science. The new direct measurements confirm all previous indirect results. Through a reduced uncertainty of the mass of ^{55}V we confirm the quenching of the $N = 32$ neutron shell closure in vanadium. We discuss the evolution of the $N = 32$ neutron shell closure between K and Cr and show similar signatures in the half-life surface when studied along the isotopic chains.

I. INTRODUCTION

The internal structure of the nucleus, a finite quantum system of protons and neutrons, manifests itself in the occurrence of nuclear shells at the well known magic numbers 2, 8, 20, 28, 50, 82, and 126 [1]. Here, due to large energy gaps in the single-particle orbitals, unique patterns in the otherwise smooth nuclear observables appear when studied across the nuclear chart [2]. High-precision mass measurements allow a determination of the binding energy, reflecting the sum of all interactions within the nucleus and allowing calculation of the one- and two-nucleon separation energies. Unique signatures in these differential quantities indicate that closed-shell nuclei are more bound compared to open-shell systems [3]. Many nuclear properties, in particular the particle-emission probabilities and half-lives, depend on the available energy and phase-space of the decay. They are, therefore, affected by sudden changes in the total binding energy caused by changes in the nuclear structure.

It has become evident that the structure of the nucleus can change away from the valley of β stability [4], where new phenomena, e.g., shell quenching, weakening, or disappearance of shells at the classical magic numbers, appearance of new magic numbers have been theoretically predicted and experimentally observed [5,6]. Of great interest has been the emergence of the $N = 32$ neutron shell closure [7], that was first predicted from self-consistent energy density functional calculations [8] and experimentally validated by measurements of the first excited 2^+ states in neutron-rich $_{20}$Ca [9]. Within the picture of tensor-force-driven shell evolution it forms by a weakening of the attractive nucleon-nucleon force between the proton $\pi f_{7/2}$ and the neutron $\nu f_{5/2}$ single-particle orbitals due to reduced proton numbers in the $\pi f_{7/2}$ orbital [10].

In this region Penning-trap mass measurements by ISOLTRAP [11,12] and TRIUMF's Ion Trap for Atomic and Nuclear science (TITAN) [13] show strong shell effects in neutron rich $_{19}$K and $_{20}$Ca isotopes at $N = 32$. Similar behavior has been seen for $_{21}$Sc in mass measurements at the CSRe storage ring [14]. Recent work at TITAN [15] showed the transitional behavior in the $_{22}$Ti isotopic chain along the $N = 32$ isotone in comparison to state-of-the-art *ab initio* shell model calculations. By contrast, in $_{24}$Cr [16] and $_{23}$V no shell effects can be seen at $N = 32$. Despite intense work in this
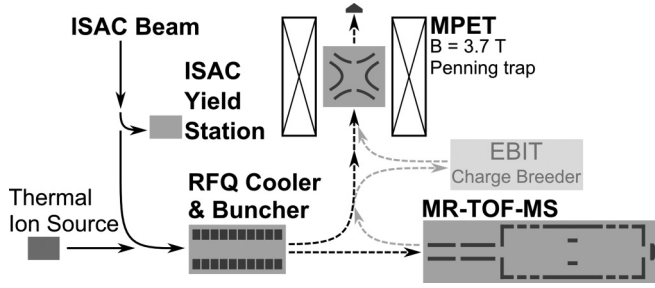

FIG. 1. Overview of the experimental facilities described herein: The ISAC yield station and TITAN for mass measurements. TITAN's individual subsystems, an RFQ Cooler and Buncher, an MR-TOF-MS, an EBIT and the measurement Penning trap MPET are shown. Continuous ion beams are indicated by solid arrows, whereas bunched beams are shown by dashed arrows.

region of the nuclear chart, the masses of neutron-rich $_{23}$V isotopes remain the only mass values around $N = 32$ purely based on indirect techniques (nuclear reactions [17–20] and decay measurements [21–24]) within the AME2016 [25].

In order to examine the aforementioned trends for isotopes with $N = 32$ neutrons we performed precision mass measurements of neutron-rich $_{23}$V isotopes at TITAN. The results presented here are part of a larger measurement campaign investigating the $N = 32$ neutron shell closure, where mass values of neutron-rich $_{22}$Ti isotopes have been published in [15], but further technical and experimental details will be discussed here.

II. EXPERIMENTAL DESCRIPTION

The radioactive isotopes were produced at TRIUMF's isotope separator and accelerator (ISAC) facility [26] in a low-power tantalum target by a 480 MeV, 40μA proton beam.

From the target extracted isotopes of $_{25}$Mn, $_{24}$Cr, and $_{23}$V were surface-ionized using a rhenium surface ion source, whereas $_{22}$Ti isotopes were additionally ionized using a two-step resonant ionization laser scheme [27] by TRIUMF's laser ionization source (TRILIS) [28]. The composite beam, dominated by stable $_{24}$Cr isotopes, was mass separated by ISAC's mass separator [29] and delivered consecutively to the ISAC yield station [30] and to TITAN [31]. A schematic of the experiment is given in Fig. 1.

At TITAN the continuous radioactive beam was accumulated, cooled and bunched in TITAN's helium-gas-filled radio frequency quadrupole (RFQ) cooler-buncher [32,33]. Cold ion bunches were sent to either the multiple-reflection time-of-flight mass-Spectrometer and isobar separator (MR-TOF-MS) [34] or the measurement Penning trap (MPET) [35], which were operated independently in this experiment. The electron beam ion trap (EBIT) [36] was not used in this experiment. The MR-TOF-MS was used to determine the RIB composition and for mass measurements of all beam species with mass number A between 51 and 55. MPET was used to measure the masses of $^{51–53}$Ti$^+$ and the respective MR-TOF-MS isobaric calibration ions ^{51}V$^+$ and $^{52–54}$Cr$^+$. The relevant subsystems are described in more detail in the following section.
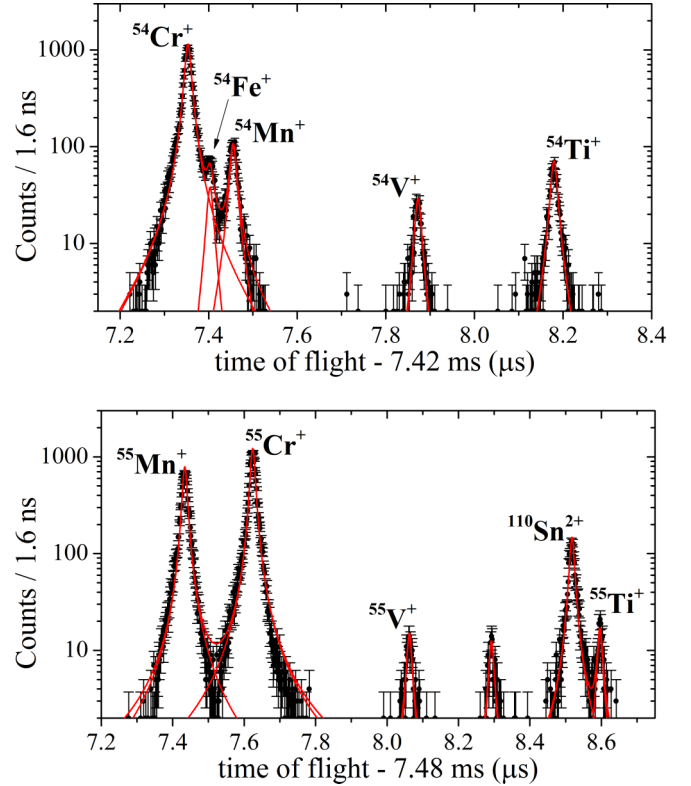

FIG. 2. Typical MR-TOF-MS time-of-flight spectra for ^{54}V$^+$ (top) and ^{55}V$^+$ (bottom) after 512 isochronous turns inside the mass analyzer of the MR-TOF-MS. The red line shows a fit to the data using Lorentz peak shapes.

A. Mass measurements at MR-TOF-MS

In the MR-TOF-MS the mass is determined via the time-of-flight method [37,38]. Long time of flights are achieved by storing an ion bunch between two electrostatic isochronous ion mirrors preserving the initial time spread over a large flight path [39], while keeping the overall dimensions of the device compact. The TITAN MR-TOF-MS has been built at the JLU-Giessen and is based on the design of the system used at GSI, Darmstadt [40,41]. It consists of a helium-gas-filled RFQ-based low-energy transport system [42] including a dedicated RF injection trap and an electrostatic time-of-flight mass analyzer [43]. In this experiment the MR-TOF-MS was operated at a 20 ms cycle time. Ions from the RFQ cooler-buncher were injected into the transport system and transported to the RF injection trap. After a cooling period of ≈ 13 ms the ions were injected into the mass analyzer and underwent 512 isochronous turns before impinging on a microchannel plate (MCP) detector. The time-of-flight focus was aligned with the MCP detector using a time-focus-shift (TFS) turn [44] prior to the isochronous reflections. The individual species produced ion bunches with peak width of about 17 ns FWHM after time of flights of about 7.4 ms, corresponding to mass resolving power of $\approx 220\,000$. The obtained peaks at the MR-TOF-MS, see Fig. 2, are symmetric and the central part is Gaussian like, whereas the tails can be described by Lorentzian line shapes for about ≈ 2.5 order of magnitude.

TABLE I. Mass excess (ME) of neutron-rich $^{52-55}$V isotopes determined by the TITAN MR-TOF-MS in comparison to the AME2016 value [25]. Our direct measurements of singly charged ions are compared to prior methods. The isobaric calibrant used for the mass measurement of each species are listed.

Species	Calibrant	ME$_{\text{TITAN}}$ (keV)	ME$_{\text{AME16}}$ [25] (keV)	Difference (keV)	Previous method & Ref.
^{52}V	^{52}Cr	$-51417(26)$	$-51443.8(0.4)$	$-27(26)$	(^{3}He, p)[17] (n,γ)[47] (d, p)[48]
^{53}V	^{53}Cr	$-51851(19)$	$-51851(3)$	$0(20)$	β[22] (t, p)[18] (d, ^{3}He)[19]
^{54}V	^{54}Cr	$-49904(17)$	$-49893(15)$	$11(22)$	β[23,24] (t, ^{3}He)[19]
^{55}V	^{55}Cr	$-49125(27)$	$-49140(100)$	$-15(104)$	β[20,24]

The time-of-flight spectra are calibrated using a calibration function according to

$$m/q = c(t - t_0)^2 \qquad (1)$$

with calibration parameters c and t_0, the mass m and charge q, and t the time of flight of the ion of interest. The parameter c is a device-specific calibration parameter and depends on the kinetic energy of the ions and the path length of the time-of-flight system and, hence, on the number of isochronous turns. The time offset t_0 is caused by signal propagation times and electronic delays; therefore, it is constant for a given experiment and data acquisition system. $t_0 = 111(4)$ ns was determined from a dedicated measurement of the time of flight t_{ref} and known mass-to-charge $m_{\text{ref}}/q_{\text{ref}}$ of ^{39}K$^+$ and ^{41}K$^+$, taken from [25], undergoing one TFS turn. The calibration parameter c was determined using a well-known isobaric reference ion present in the radioactive beam, typically a stable isobar, listed in Table I, undergoing the same number of turns as the ion of interest. In order to account for time-dependent drifts and fluctuations caused by the electronics a time-dependent calibration according to [45] using Eq. (1) was performed.

The influence of the fitting function on the mass value was investigated using the high-statistics peak of ^{52}Cr$^+$. For this well-separated peak deviations of the centroid, resulting from fitting with a Gaussian or Lorentzian peak shape to the same data, were determined to be within $\Delta m/m < 5 \times 10^{-8}$. To account for peak shape dependent effects, in particular for nearby or overlapping peaks, two independent analyses were performed, using Gaussian and Lorentzian peak shapes. The same peak width was applied to all peaks within one spectra during fitting.

The error on the mass value for each species was taken from the fitting algorithm and quadratically added to: (i) a purely statistical error $\sigma/\sqrt{(N)}$ for Gaussian [FWHM/$\sqrt{(N)}$ for Lorentzian], where σ (FWHM) corresponds to the standard deviation (FWHM) of the peak and N to the number of events recorded, (ii) the uncertainty of the calibration peak and its uncertainty reported in the AME2016 [25], and (iii) a systematic uncertainty of $\delta m/m_{\text{syst}} = 3 \times 10^{-7}$ [46]. The systematic uncertainty has been determined as an upper limit systematic uncertainty for the MR-TOF-MS from accuracy measurements before and after this experiment of ^{39}K$^+$ and ^{41}K$^+$ and is dominated by the effects of an electric ringing resulting from switching of the second ion mirror for ejection of the ions. Systematic uncertainties arising from possible ion-ion interaction inside the mass analyzer are negligible as

the measurements were performed with less than one ion per cycle.

The final mass value and uncertainty was taken as the unweighted average of the two individual analyses, which agreed on average within 0.13 standard deviations. The results are reported in Table I and compared to the values reported in AME2016 [25]. An average relative uncertainty of $\delta m/m = 4 \times 10^{-7}$ was obtained for the masses of neutron-rich V isotopes using the TITAN MR-TOF-MS.

B. Mass measurements at MPET

TITAN's MPET [35] is a precision Penning trap system housed in a homogeneous 3.7 T superconducting magnet. With MPET the mass is determined by a measurement of the ion's cyclotron frequency, described by

$$\nu_c = \frac{qB}{2\pi m} \qquad (2)$$

with m and q being the mass and charge of the ion and B the magnetic field. For the measurement of ν_c the well established time-of-flight ion-cyclotron-resonance technique (ToF-ICR) [49] was used.

In total three distinct RF excitations were applied for preparation of the ion bunch, removal of contaminants, and measurement of the cyclotron frequency. (i) A dipolar excitation was used to excite all ions' magnetron motion. (ii) A single square-shaped dipole pulse at the reduced cyclotron frequency of each contaminant species, previously identified by the MR-TOF-MS, was used to move contaminant species out of the interaction region with the ion of interest. (iii) A quadrupole RF excitation part of the ToF-ICR measurement of the cyclotron frequency [50]. Total preparation times of 60–70 ms were employed for (i) and (ii).

To calibrate the magnetic field B and to account for time-dependent fluctuations, measurements of the ν_c of the ion of interest were interleaved with calibration measurements of the $\nu_{c,\text{ref}}$ of ^{39}K$^+$ ions.

The atomic mass M is calculated from the cyclotron frequency ratio R between the species of interest and the reference ion

$$R = \frac{\nu_{c,\text{ref}}}{\nu_c} = \frac{(M - m_e)}{(M_{\text{ref}} - m_e)} \qquad (3)$$

and the atomic mass of the reference ion M_{ref}. Three standard [50] or Ramsey-type [51] measurements of the frequency ratio between the ion of interest and the calibration species were employed with excitation times between 100 and 250 ms
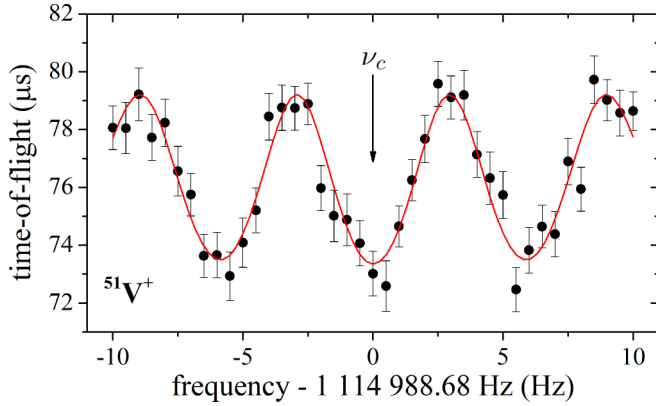
FIG. 3. Typical ToF-ICR resonance from MPET for ^{51}V$^+$ achieved with a 40-120-40 ms Ramsey-type excitation scheme containing 940 counts. The solid line shows a fit to the data with the theoretical line shape [49].

allowing for a mass determination of the ion of interest with precisions $\delta m/m$ of $\sim 10^{-8}$. A typical Ramsey resonance of ^{51}V$^+$ is shown in Fig. 3 using a 40-120-40 ms (on-off-on) excitation scheme.

Systematic uncertainties, described in detail in [35,52], arising, e.g., from ion-ion interaction, time-dependent magnetic field fluctuations, and the decay of the magnetic field, as well as field alignment were investigated, following the approach therein. These systematic uncertainties were calculated to be one to two orders of magnitude lower than the statistical uncertainty of each cyclotron frequency measurement and, thus, negligible. In order to limit possible ion-ion effects further, only bunches with one or two detected ions were used for the determination of the frequency ratios. Mass-dependent effects were studied by performing a reference measurement of ^{85}Rb$^+$ and found to be smaller than 1.5×10^{-8} for the masses of interest. This upper limit systematic uncertainty was added quadratically to obtain the final uncertainty. The average frequency ratios obtained with MPET for singly charged ^{51}V and $^{51-53}$Ti are given in Table II as well as the mass excess, first reported in [15]. In addition we performed measurements of stable $^{52-54}$Cr, the calibration species of the MR-TOF-MS measurements. Our results are in good agreement with the

TABLE II. Average MPET frequency ratios for singly charged Cr, V, and Ti ions and mass excess (ME) of the atomic species. All measurements are calibrated with ^{39}K$^+$, using values taken from AME2016 [25].

Species	ME$_{\text{TITAN}}$ (atomic) (keV)	$\bar{R}$ (ion)
^{52}Cr	−55421.3 (2.0)	1.333052991(55)
^{53}Cr	−55288.4 (1.9)	1.358721924(52)
^{54}Cr	−56929.3 (4.6)	1.384341984(130)
^{51}V	−52203.5 (1.8)	1.307476380(50)
^{51}Ti	−49731.5 (2.1)	1.307544491(58)
^{52}Ti	−49479.1 (3.0)	1.333216716(83)
^{53}Ti	−46881.4 (2.9)	1.358953560(80)

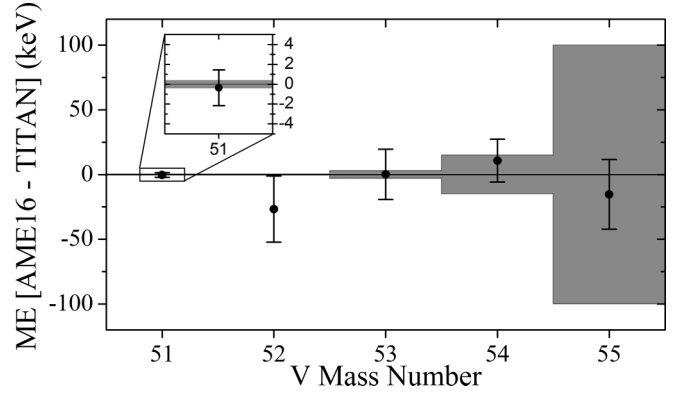FIG. 4. Difference in mass excess of $_{23}$V between the value reported in AME2016 and this work, the AME2016 uncertainty is shown as a gray band. The mass excess of ^{51}V was determined by MPET, whereas $^{52-55}$V were measured by the MR-TOF-MS.

AME2016 [25] and with recent mass measurements by LEBIT [53].

III. DISCUSSION

In Fig. 4 the new vanadium mass excesses determined from our direct mass measurements are compared to the averages reported in the AME2016 [25]. The previous measurements relying upon nuclear reactions [17–20] and decay measurements [21–24] are confirmed by our direct mass measurements of $A = 52$–55 V isotopes. For ^{54}V we were able to reach a comparable uncertainty and for ^{55}V it was possible to reduce the uncertainty by a factor of ≈ 4, down to 27 keV.

Based on these new mass values M we calculate the two-neutron separation energy S_{2n} of neutron-rich $_{23}$V as

$$S_{2n}(N, Z) = M(Z, N - 2) + 2M_n - M(N, Z) \qquad (4)$$

with M_n the mass of a neutron, shown in Fig. 5 in addition to S_{2n} values based on our recent Ti [15] mass measurements and known values reported in the AME2016. A clear change in behavior along the $N = 32$ isotone can be seen. Whereas in $_{19}$K, $_{20}$Ca, and $_{21}$Sc very dominant shell effects are present as seen by the steep drop in S_{2n}, this change in slope flattens out in $_{22}$Ti and completely vanishes in $_{23}$V and $_{24}$Cr. The new TITAN measurements with reduced uncertainties for $_{22}$Ti and $_{23}$V reveal the presence of a very weak shell closure in $_{22}$Ti and clearly indicate the absence of a $N = 32$ shell closure in $_{23}$V.

This can be seen more clearly in the trends of the empirical shell gap Δ_{2n}, defined by

$$\Delta_{2n}(Z, N) = S_{2n}(Z, N) - S_{2n}(Z, N + 2), \qquad (5)$$

which highlights closed shell effect, shown for $_{23}$V and $_{20}$Ca in Fig. 6. The direct high-precision data show a shell gap of ≈ 4.6 MeV at $N = 28$ in $_{23}$V, which is comparable to the shell gap in $_{20}$Ca of ≈ 5.7 MeV at the same neutron number and reveals the presence of a strong $N = 28$ neutron shell closure in both isotopic chains.

For $N = 32$ the empirical shell gap shows a different behavior for $_{20}$Ca and $_{23}$V. In $_{23}$V a flat baseline around ≈ 2 MeV can
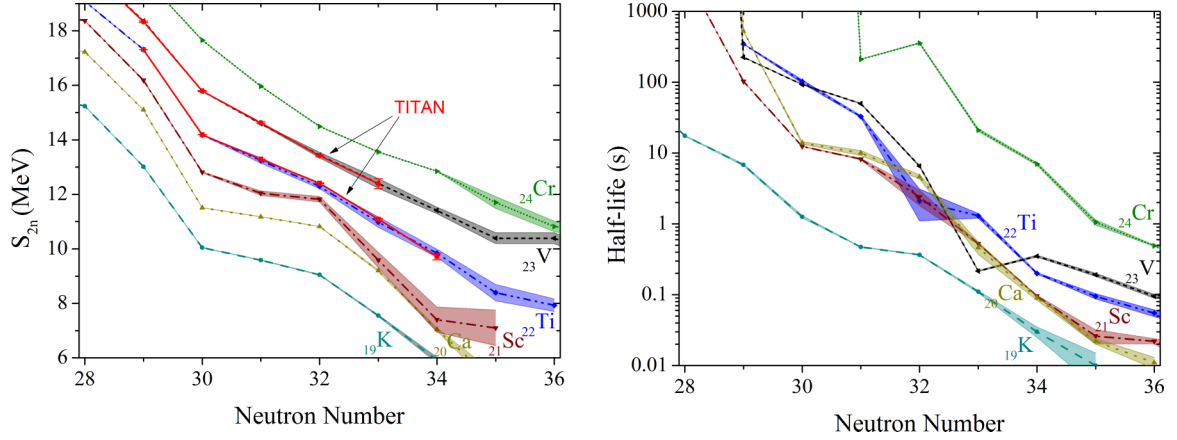
FIG. 5. (Left) S_{2n} values and uncertainties (shown as bands) of $Z = 19$ to $Z = 24$ isotopes around the $N = 32$ neutron shell closure, data taken from [25]. S_{2n} values including the new $_{23}$V (this work) and $_{22}$Ti ([15]) masses (shown as red symbols) clearly confirm a quenching of the $N = 32$ between Sc to V, with Ti being the transition between strong and no shell effects. (Right) Half-lives and their uncertainties (shown as bands) of $Z = 19$ to $Z = 24$ isotopes around the $N = 32$ shell closure, taken from [54]. A change in slope in the otherwise smooth trend within the $_{20}$Ca and $_{21}$Sc half-lives approaching $N = 32$ can be seen, matching clear shell effects seen in the S_{2n} values.

be seen, whereas in $_{20}$Ca a shell gap of ≈ 3.8 MeV indicates the presence of a $N = 32$ shell closure. Thus confirming the absence of closed shell structures in $_{23}$V around $N = 32$ and the complete quenching of the $N = 32$ neutron shell closure seen by mass measurements.

Previous spectroscopic studies identified high first excited 2^+ states $E(2_1^{2+})$ in even-even nuclides of $_{20}$Ca, $_{22}$Ti, and even $_{24}$Cr [54] as well as low-lying yrast sates in $_{23}$V [55,56]. These studies suggest an extension of the $N = 32$ neutron shell closure, possibly up to $_{24}$Cr. Low-statistics γ and β spectroscopy were performed at the ISAC Yield Station [30] prior to the mass measurements herein. The results hint at a longer half-life for ^{54}Ti and new transitions than found in previous studies [24,57]. A nuanced understanding calls for dedicated spectroscopy in this region of the nuclear chart.

Nevertheless comparing the evolution of the half-lives following each isotopic chain around $N = 32$ (see Fig. 5) we find a clear change in behavior for the $_{20}$Ca and $_{21}$Sc

isotopic chains approaching $N = 32$, compared the otherwise smooth trend seen in the half-life surface. The half-life of an isotope strongly depends on the Q value of the associated decay channel, therefore rapid changes in the binding energy caused by changes in the underlying nuclear structure may also manifest in the half-life when studied across isotopic chains. These changes are convoluted with changes in spin and parity of the mother and daughter nucleus and are therefore in general less pronounced. For $_{20}$Ca and $_{21}$Sc a rapid change in slope can be seen at $N = 30$ towards isotopes with $N = 32$ neutrons, showing that $N = 32$ $_{20}$Ca and $_{21}$Sc isotopes are comparably longer lived than expected from the trend. This structure manifesting in the half-life surface matches the signatures seen in the S_{2n} surface, where $_{20}$Ca and $_{21}$Sc show strong shell effects, and suggesting to result from a rapid changes in binding energy and an increased magicity.

IV. CONCLUSION

In summary, we performed the first direct mass measurements of neutron-rich vanadium isotopes with TITAN's newly installed MR-TOF-MS and discuss details about the experiment and analysis, resulting in an average relative uncertainty of $\delta m/m = 4 \times 10^{-7}$ for the masses of neutron-rich vanadium. The new mass values of $^{51-55}$V agree well within one standard deviation with the previous values reported in the AME2016 [25] purely based on indirect measurements. By reducing the uncertainty of ^{55}V with the first direct mass measurement, no significant shell effects can be observed in the V isotopic chain in either the S_{2n} or Δ_{2n} surfaces and the full quenching of the $N = 32$ neutron shell closure in vanadium is confirmed as seen by mass measurements.
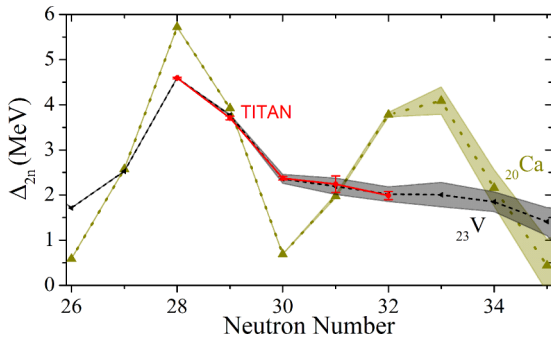

FIG. 6. Empirical neutron-shell gap Δ_{2n} for the $_{23}$V and $_{20}$Ca isotopic chain. Values based on the direct mass measurements of $_{23}$V reported here in addition to values and uncertainties based on the AME2016 [25] shown as a band. The direct measurements affirm the absence and quenching of the $N = 32$ neutron shell closure in $_{23}$V in comparison to $_{20}$Ca showing strong shell effects at $N = 32$.

[1] M. Goeppert Mayer and J. H. Jensen, *Elementary Theory of Nuclear Shell Structure* (John Wiley and Sons, New York, 1955).

[2] I. Bentley, Y. C. Rodríguez, S. Cunningham, and A. Aprahamian, Phys. Rev. C **93**, 044337 (2016).

[3] A. Bohr and B. R. Mottelson, *Nuclear Structure, Single Particle Motion* (WA Benjamin Inc., New York, 1969), Vol. 1.

[4] D. Warner, Nature **430**, 517 (2004).

[5] O. Sorlin and M. G. Porquet, Prog. Part. Nucl. Phys. **61**, 602 (2008).

[6] R. Kanungo, Phys. Scr. **2013**, 014002 (2013).

[7] D. Steppenbeck, S. Takeuchi, N. Aoi, P. Doornenbal, M. Matsushita, H. Wang, H. Baba, N. Fukuda, S. Go, M. Honma, J. Lee, K. Matsui, S. Michimasa, T. Motobayashi, D. Nishimura, T. Otsuka, H. Sakurai, Y. Shiga, P.-a. Söderström, T. Sumikama, H. Suzuki, R. Taniuchi, Y. Utsuno, J. J. Valiente-Dobón, and K. Yoneda, Nature **502**, 207 (2013).

[8] F. Tondeur, *Proceedings of the 4th International Conference on Nuclear Far from Stability, Helsingør, Denmark* (Cern, Geneva, 1981), pp. 81–89.

[9] A. Huck, G. Klotz, A. Knipper, C. Miehé, C. Richard-Serre, G. Walter, A. Poves, H. L. Ravn, and G. Marguier, Phys. Rev. C **31**, 2226 (1985).

[10] T. Otsuka, T. Suzuki, R. Fujimoto, H. Grawe, and Y. Akaishi, Phys. Rev. Lett. **95**, 232502 (2005).

[11] F. Wienholtz, D. Beck, K. Blaum, C. Borgmann, M. Breitenfeldt, R. B. Cakirli, S. George, F. Herfurth, J. D. Holt, M. Kowalska, S. Kreim, D. Lunney, V. Manea, J. Menéndez, D. Neidherr, M. Rosenbusch, L. Schweikhard, A. Schwenk, J. Simonis, J. Stanja, R. N. Wolf, and K. Zuber, Nature **498**, 346 (2013).

[12] M. Rosenbusch, P. Ascher, D. Atanasov, C. Barbieri, D. Beck, K. Blaum, C. Borgmann, M. Breitenfeldt, R. B. Cakirli, A. Cipollone, S. George, F. Herfurth, M. Kowalska, S. Kreim, D. Lunney, V. Manea, P. Navrátil, D. Neidherr, L. Schweikhard, V. Somà, J. Stanja, F. Wienholtz, R. N. Wolf, and K. Zuber, Phys. Rev. Lett. **114**, 202501 (2015).

[13] A. T. Gallant, J. C. Bale, T. Brunner, U. Chowdhury, S. Ettenauer, A. Lennarz, D. Robertson, V. V. Simon, A. Chaudhuri, J. D. Holt, A. A. Kwiatkowski, E. Mané, J. Menéndez, B. E. Schultz, M. C. Simon, C. Andreoiu, P. Delheij, M. R. Pearson, H. Savajols, A. Schwenk, and J. Dilling, Phys. Rev. Lett. **109**, 032506 (2012).

[14] X. Xu, M. Wang, Y. H. Zhang, H. S. Xu, P. Shuai, X. L. Tu, Y. A. Litvinov, X. H. Zhou, B. H. Sun, Y. J. Yuan, J. W. Xia, J. C. Yang, K. Blaum, R. J. Chen, X. C. Chen, C. Y. Fu, Z. Ge, Z. G. Hu, W. J. Huang, D. W. Liu, Y. H. Lam, X. W. Ma, R. S. Mao, T. Uesaka, G. Q. Xiao, Y. M. Xing, T. Yamaguchi, Y. Yamaguchi, Q. Zeng, X. L. Yan, H. W. Zhao, T. C. Zhao, W. Zhang, and W. L. Zhan, Chin. Phys. C **39**, 104001 (2015).

[15] E. Leistenschneider, M. P. Reiter, S. Ayet San Andrés, B. Kootte, J. J. D. Holt, P. Navrátil, C. Babcock, C. Barbieri, B. R. B. Barquest, J. Bergmann, J. Bollig, T. Brunner, E. Dunling, A. Finlay, H. Geissel, L. Graham, F. Greiner, H. Hergert, C. Hornung, C. Jesch, R. Klawitter, Y. Lan, D. Lascar, K. K. G. Leach, W. Lippert, J. E. J. McKay, S. F. S. Paul, A. Schwenk, D. Short, J. Simonis, V. Somà, R. Steinbrügge, S. R. S. Stroberg, R. Thompson, M. M. E. Wieser, C. Will, M. Yavor, C. Andreoiu, T. Dickel, I. Dillmann, G. Gwinner, W. W. R. Plaß, C. Scheidenberger, A. A. A. Kwiatkowski, and J. Dilling, Phys. Rev. Lett. **120**, 062503 (2018).

[16] C. Guénaut, G. Audi, D. Beck, K. Blaum, G. Bollen, P. Delahaye, F. Herfurth, A. Kellerbauer, H. J. Kluge, D. Lunney, S. Schwarz, L. Schweikhard, and C. Yazidjian, J. Phys. G: Nucl. Part. Phys. **31**, S1765 (2005).

[17] T. Caldwell, D. Pullen, and O. Hansen, Nucl. Phys. A **242**, 221 (1975).

[18] S. Hinds, H. Marchant, and R. Middleton, Phys. Lett. B **24**, 34 (1967).

[19] E. R. Flynn, J. W. Sunier, and F. Ajzenberg-Selove, Phys. Rev. C **15**, 879 (1977).

[20] A. M. Nathan, D. E. Alburger, J. W. Olness, and E. K. Warburton, Phys. Rev. C **16**, 1566 (1977).

[21] W. Köhler and K. Knopf, Zeitschrift für Naturforsch. A **20**, 969 (1965).

[22] L. A. Parks, C. N. Davids, and R. C. Pardo, Phys. Rev. C **15**, 730 (1977).

[23] T. Ward, P. Pile, and P. Kuroda, Nucl. Phys. A **148**, 225 (1970).

[24] T. Dörfler, W.-D. Schmidt-Ott, T. Hild, T. Mehren, W. Böhmer, P. Möller, B. Pfeiffer, T. Rauscher, K.-L. Kratz, O. Sorlin, V. Borrel, S. Grévy, D. Guillemaud-Mueller, A. C. Mueller, F. Pougheon, R. Anne, M. Lewitowicz, A. Ostrowsky, M. Robinson, and M. G. Saint-Laurent, Phys. Rev. C **54**, 2894 (1996).

[25] M. Wang, G. Audi, F. G. Kondev, W. Huang, S. Naimi, and X. Xu, Chin. Phys. C **41**, 030003 (2017); L. Vinet and A. Zhedanov, J. Phys. A: Math. Theor. **44**, 085201 (2011).

[26] G. C. Ball, G. Hackman, and R. Krücken, Phys. Scr. **91**, 093002 (2016).

[27] T. Takamatsu, H. Tomita, T. Furuta, T. Takatsuka, Y. Adachi, T. Noto, V. Sonnenschein, T. Kron, K. Wendt, T. Iguchi, T. Sonoda, and M. Wada, JPS Conf. Proc. **6**, 030142 (2015).

[28] J. Lassen, P. Bricault, M. Dombsky, J. P. Lavoie, M. Gillner, T. Gottwald, F. Hellbusch, A. Teigelhöfer, A. Voss, and K. D. A. Wendt, AIP Conf. Proc. **1104**, 9 (2009).

[29] P. Bricault, R. Baartman, M. Dombsky, A. Hurst, C. Mark, G. Stanford, and P. Schmor, Nucl. Phys. A **701**, 49 (2002).

[30] P. Kunz, C. Andreoiu, P. Bricault, M. Dombsky, J. Lassen, A. Teigelhöfer, H. Heggen, and F. Wong, Rev. Sci. Instrum. **85**, 053305 (2014).

[31] J. Dilling, R. Baartman, P. Bricault, M. Brodeur, L. Blomeley, F. Buchinger, J. Crawford, J. R. Crespo López-Urrutia, P. Delheij, M. Froese, G. P. Gwinner, Z. Ke, J. K. P. Lee, R. B. Moore, V. Ryjkov, G. Sikler, M. Smith, J. Ullrich, and J. Vaz, Int. J. Mass Spectrom. **251**, 198 (2006).

[32] M. Smith, L. Blomeley, P. Delheij, and J. Dilling, Hyperfine Interact. **173**, 171 (2006).

[33] T. Brunner, M. J. Smith, M. Brodeur, S. Ettenauer, A. T. Gallant, V. V. Simon, A. Chaudhuri, A. Lapierre, E. Mané, R. Ringle, M. C. Simon, J. A. Vaz, P. Delheij, M. Good, M. R. Pearson, and J. Dilling, Nucl. Instrum. Methods Phys. Res. A **676**, 32 (2012).

[34] C. Jesch, T. Dickel, W. R. Plass, D. Short, S. Ayet San Andres, J. Dilling, H. Geissel, F. Greiner, J. Lang, K. G. Leach, W. Lippert, C. Scheidenberger, and M. I. Yavor, Hyperfine Interact. **235**, 97 (2015).

[35] M. Brodeur, V. L. Ryjkov, T. Brunner, S. Ettenauer, A. T. Gallant, V. V. Simon, M. J. Smith, A. Lapierre, R. Ringle, P. Delheij, M. Good, D. Lunney, and J. Dilling, Int. J. Mass Spectrom. **310**, 20 (2012).

[36] A. Lapierre, M. Brodeur, T. Brunner, S. Ettenauer, A. T. Gallant, V. Simon, M. Good, M. W. Froese, J. R. Crespo Lpez-Urrutia, P. Delheij, S. Epp, R. Ringle, S. Schwarz, J. Ullrich, and J. Dilling, Nucl. Instrum. Methods Phys. Res. A **624**, 54 (2010).

[37] A. E. Cameron and D. F. Eggers, Rev. Sci. Instrum. **19**, 605 (1948).

[38] W. C. Wiley and I. H. McLaren, Rev. Sci. Instrum. **26**, 1150 (1955).

[39] H. Wollnik and M. Przewloka, Int. J. Mass Spectrom. Ion Process. **96**, 267 (1990).

[40] W. R. Plass, T. Dickel, U. Czok, H. Geissel, M. Petrick, K. Reinheimer, C. Scheidenberger, and M. I.Yavor, Nucl. Instrum. Methods Phys. Res. B **266**, 4560 (2008).

[41] T. Dickel, W. R. Plass, A. Becker, U. Czok, H. Geissel, E. Haettner, C. Jesch, W. Kinsel, M. Petrick, C. Scheidenberger, A. Simon, and M. I. Yavor, Nucl. Instrum. Methods Phys. Res. A **777**, 172 (2015).

[42] W. R. Plass, T. Dickel, S. A. S. Andres, J. Ebert, F. Greiner, C. Hornung, C. Jesch, J. Lang, W. Lippert, T. Majoros, D. Short, H. Geissel, E. Haettner, M. P. Reiter, A.-K. Rink, C. Scheidenberger, and M. I. Yavor, Phys. Scr. **T166**, 014069 (2015).

[43] M. I. Yavor, W. R. Plass, T. Dickel, H. Geissel, and C. Scheidenberger, Int. J. Mass Spectrom. **381–382**, 1 (2015).

[44] T. Dickel, M. I. Yavor, J. Lang, W. R. Plass, W. Lippert, H. Geissel, and C. Scheidenberger, Int. J. Mass Spectrom. **412**, 1 (2017).

[45] J. Ebert, Mass Measurements of U-Projectile Fragments for the First Time with a Multiple-Reflection Time-Of-Flight Mass Spectrometer, Ph.D. thesis, University of Giessen (2016).

[46] C. Will, TITAN's Multiple-Reflection Time-of-Flight Mass Spectrometer and Isobar Separator - Characterization and First Experiments, B.sc. thesis, University of Giessen (2017).

[47] J. de Haas, K. Abrahams, T. Tielens, H. Postma, and W. Huiskamp, Nucl. Phys. A **419**, 101 (1984).

[48] A. Sperduto and W. W. Buechner, in *Proceedings of the International Conference on Nuclidic Masses,* edited by W. H. Johnson, Jr., (Springer-Verlag, Vienna, 1964), p. 289.

[49] M. König, G. Bollen, H.-J. Kluge, T. Otto, and J. Szerypo, Int. J. Mass Spectrom. Ion Process. **142**, 95 (1995).

[50] M. Kretzschmar, Int. J. Mass Spectrom. **349–350**, 227 (2013).

[51] S. George, S. Baruah, B. Blank, K. Blaum, M. Breitenfeldt, U. Hager, F. Herfurth, A. Herlert, A. Kellerbauer, H.-J. Kluge, M. Kretzschmar, D. Lunney, R. Savreux, S. Schwarz, L. Schweikhard, and C. Yazidjian, Phys. Rev. Lett. **98**, 162501 (2007).

[52] M. Brodeur, T. Brunner, C. Champagne, S. Ettenauer, M. Smith, A. Lapierre, R. Ringle, V. L. Ryjkov, G. Audi, P. Delheij, D. Lunney, and J. Dilling, Phys. Rev. C **80**, 044318 (2009).

[53] R. M. E. B. Kandegedara, G. Bollen, M. Eibach, N. D. Gamage, K. Gulyuz, C. Izzo, M. Redshaw, R. Ringle, R. Sandler, and A. A. Valverde, Phys. Rev. C **96**, 044321 (2017).

[54] M. R. Bhat, Evaluated Nuclear Structure Data File (ENSDF), *Nuclear Data for Science and Technology*, edited by S. M. Qaim (SpringerVerlag, Berlin, Germany, 1992), p. 817.

[55] D. R. N. for the Clara-Prisma collaboration, J. Phys. Conf. Ser. **49**, 91 (2006).

[56] S. Lunardi, AIP Conf. Proc. **1120**, 70 (2009).

[57] H. L. Crawford, R. V. F. Janssens, P. F. Mantica, J. S. Berryman, R. Broda, M. P. Carpenter, N. Cieplicka, B. Fornal, G. F. Grinyer, N. Hoteling, B. P. Kay, T. Lauritsen, K. Minamisono, I. Stefanescu, J. B. Stoker, W. B. Walters, and S. Zhu, Phys. Rev. C **82**, 014311 (2010).